JACOBS
UNIVERSITY

Ray Tracing of an Accelerated Constructive Solid Geometry Algorithm

by

Otmane Sabir

Bachelor Thesis in Computer Science

Submission: April 11, 2021 Supervisor: Prof. Dr. Sergey Kosov

Jacobs University Bremen | Department of Computer Science and Electrical Engineering

English: Declaration of Authorship

I hereby declare that the thesis submitted was created and written solely by myself without any external support. Any sources, direct or indirect, are marked as such. I am aware of the fact that the contents of the thesis in digital form may be revised with regard to usage of unauthorized aid as well as whether the whole or parts of it may be identified as plagiarism. I do agree my work to be entered into a database for it to be compared with existing sources, where it will remain in order to enable further comparisons with future theses. This does not grant any rights of reproduction and usage, however.

This document was neither presented to any other examination board nor has it been published.

German: Erklärung der Autorenschaft (Urheberschaft)

Ich erkläre hiermit, dass die vorliegende Arbeit ohne fremde Hilfe ausschließlich von mir erstellt und geschrieben worden ist. Jedwede verwendeten Quellen, direkter oder indirekter Art, sind als solche kenntlich gemacht worden. Mir ist die Tatsache bewusst, dass der Inhalt der Thesis in digitaler Form geprüft werden kann im Hinblick darauf, ob es sich ganz oder in Teilen um ein Plagiat handelt. Ich bin damit einverstanden, dass meine Arbeit in einer Datenbank eingegeben werden kann, um mit bereits bestehenden Quellen verglichen zu werden und dort auch verbleibt, um mit zukünftigen Arbeiten verglichen werden zu können. Dies berechtigt jedoch nicht zur Verwendung oder VervielfÃ¤ltigung.

Diese Arbeit wurde noch keiner anderen Prüfungsbehörde vorgelegt noch wurde sie bisher veröffentlicht.

Date, Signature

Abstract

(target size: 15-20 lines)

Contents

1 Introduction

Constructive Solid Geometry (CSG) is a method used in computer graphics, computer-aided design, generic modeling languages, and numerous other applications to construct complex geometries from simple primitives or polyhedral solids through the use of boolean operators, namely union ($\cup$), difference ($-$), and intersection ($\cap$). Figure 1a through 1c respectively show intersection, union, and difference operations. The approach grows especially appealing when implemented in a ray tracing system as the core intricacy renders performing arithmetic logic on a pair of uni-dimensional rays. Nonetheless, most current ray tracing systems generally suffer from the detriment of the expensive object space intersection computation, and the generic CSG algorithms suffer immensely from their computational complexity, making it very difficult to integrate into operating rendering engines. Therefore, this research concentrates on constructive solid geometry and possible means of acceleration.

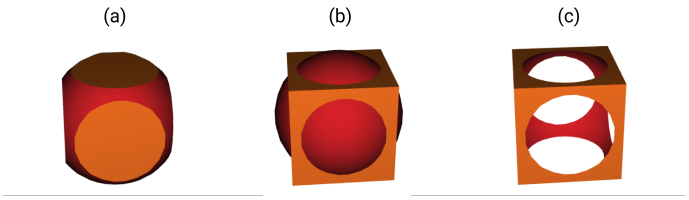

Figure 1: Examples of set operations on a mesh sphere and box.

1.1 Rendering Algorithms

Rendering digital photorealistic or non-photorealistic images has been a topic of study since the late 1960s [3]. Since then, various algorithms came forth that allow achieving different results depending on the required conditions. Inherently all these algorithms strive to solve the same underlying problem by trading-off different aspects, namely speed and realism. This problem is known as the hidden surface problem. The hidden surface problem is determining the visible objects in space from a certain point of view. There are two general methods, object-space methods, which try to start from the object space and project the geometries onto the 2D raster, or the image-space ones, which perform the opposite by tracing a ray through each pixel and attempting to locate the closest intersection of that ray with the geometries in the scene. The two methods then give birth to the pair of most famous and widely adopted rendering algorithms: rasterization and ray tracing.

1.1.1 Rasterization

Rasterization has very quickly become the dominant approach for interactive applications because of its initially low computational requirements, its massive adoption in most hardware solutions, and later by the ever-increasing performance of dedicated graphics hardware. The use of local, per-triangle computation makes it well suited for a feed-forward pipeline. However, the rasterization algorithm has many trade-offs. First, the handling of global effects, such as reflections and realistic shading, is intricate, and second, it's also limited to scenes with meshed geometries.

1.1.2 Ray Tracing

Ray tracing simulates the photographic process in reverse. For each pixel on the screen, we shoot a ray and identify objects that intersect the ray. A ray-tracing algorithm makes usage of four essential components: the camera, the geometry, the light sources, and the shaders. These components can have different varieties, to state a few, orthographic and perspective cameras, unidirectional and area light sources, and Phong and chrome shaders. Hence, it allows achieving several outcomes depending on the necessities. The main downside has been computational time and the constraints of using such an algorithm in interactive applications. However, ray tracing parallelizes efficiently and trivially. Thus it takes advantage of the continuously rising computational power of the hardware. Many applications have successfully produced real-time ray tracing algorithms and allow for highly photorealistic results in interactive applications [1, 2].

1.2 Geometric Representations

When it comes to computer graphics, we can find numerous types of geometry descriptions [5, 6, 9, 13, 16, 18]. Many solutions exist that enable the simple conversion between these geometric formats [19]. However, there are predominantly two different representations in most geometric modeling systems [16]: boundary representations - commonly known as B-Rep or BREP - and constructive solid geometry - CSG. Each one of these representations brings forward different advantages, disadvantages, and limitations.

1.2.1 Boundary Representation

Boundary representations are indirect definitions of solids in space using their boundary or limit. This representation is usually a hierarchical composition of different dimensionally complex parts. On the very top, we have definitions of two-dimensional faces, which build on uni-dimensional edges that are subsequently built on dimensionless points (See figure 2). A BREP with non-curvilinear edges and planar faces is called a polygon mesh. The points representing the edges shared by a single face must always be co-planar. A triangle is the simplest polygon and has the excellent property of always being co-planar. Additionally, polygons of any complexity are representable by a set of triangles. These qualities make triangular meshes a fundamental component in BREPs. The representations built on triangles are also highly optimized for fast operations. Therefore, we will mainly deal with triangular meshes in OpenRT, though it does offer descriptions for tetragon (quadrilateral) meshes.

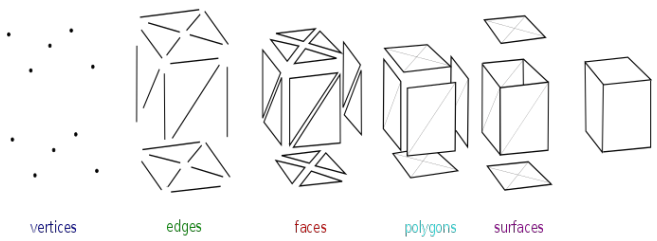

Figure 2: Sample BREP of a 3D hyper-rectangle [21]

1.2.2 Constructive Solid Geometry

Constructive solid geometry takes basis on the fundamental premise that any complex physical object is obtainable from a set of primitive geometries and the base boolean operations. CSG is radically different from BREPs as it does not collect any topological information but instead evaluates the geometries as needed by the case scenario. In other words, there is no explicit description of the boundary of the solid. Contrary to BREPs, CSG representations are quickly modified and manipulated since incremental changes do not trigger re-computation and evaluation of the boundary of a geometry. Therefore, no topological changes occur when adjusting the geometries. The latter makes it an attractive solution as it provides a high-level specification of the objects in space and permits significantly more straightforward modification and manipulation. In the general constructive solid geometry description, the solids are put in a binary tree, referred to as the CSG tree, as Figure 3 shows. The root node is the complete composite geometry. The leaf nodes depict the base geometries (cubes, spheres, cylinders, tori, cones, and polygon meshes) used in the composition. Every node in the tree, besides the leaf nodes, expresses another complete solid and contains information of the set operation of that node.

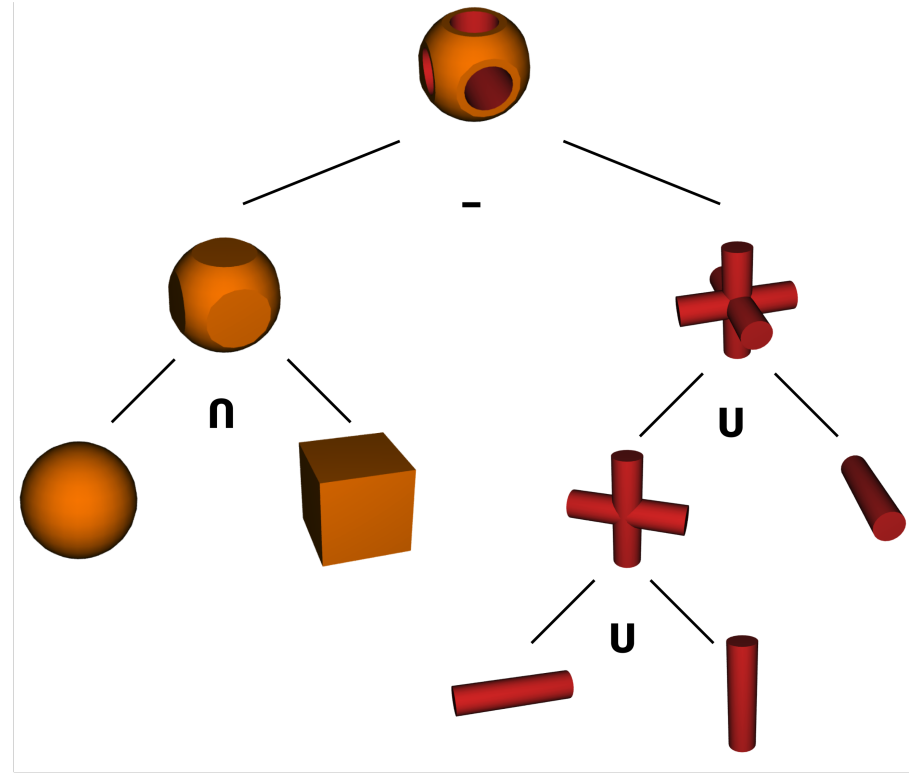

Figure 3: Basic CSG Tree

In the OpenRT library implementation, we follow a different approach to allow the use of BREPs as leaf nodes. This gives the flexibility of creating more complex geometries and allowing for nesting of combinatorial geometries inside each other. In a naive implementation, this operation is very costly; however, by using certain spatial indexing structures, each node can be represented as a binary space partitioning tree (See figure 4).

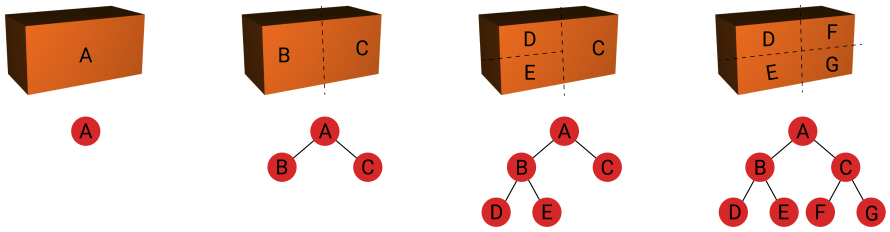

Figure 4: Sample representation of a binary space partitioning (BSP) tree.

1.3 Overview

Following this introduction, we present this CSG implementation in five sections. 2. Related Works; 3. Constructive Solid Geometry; 4. Optimization; 5. Evaluation of the results; 6. Extensions & Conclusions.

The second section presents works already done, the limitations of the proposed implementations, and solutions to problems related to CSG.

Section 3 defines the algorithm that performs the logic in the ray-tracing framework. Additionally, we introduce the data structure used to store the needed data for performing the operation, allowing transformations, and finally rendering. Additionally, we present the architecture used to enable the acceleration.

Section 4 discusses efficiency and optimizations. The visible surface problem in ray tracing requires a lot of CPU time, and without any optimizations, the CSG algorithm significantly increases the CPU pressure. Therefore, optimizations are much needed to make this method usable and suitable for real-life applications. The speed is a function of the screen resolution and the geometry complexity (how many primitives are in the solid, and the number of nested geometries).

Section 5 describes the results received from running various tests on the 3 different implementations of the algorithm. The first is the naive implementation which we refer to as NaiCSG. The second is a variant that uses a Binary Space Partition tree to solve the visible surface problem but still naively finds intersections inside the combinatorial geometry, which we will refer to as BinCSG. Lastly, we'll introduce our optimized algorithm which uses a binary space partition tree on the outside (solving the visible surface problem) and also inside each composite geometry to direct the rays towards the correct geometries, which we will refer to as OptiCSG. We conduct three types tests. The primary one is a function of time and complexity of the geometry, as we monitor the rendering time following gradual increases in the detail level of two sphere meshes. The second computes the time taken to render a scene after covering different amounts of the view port. The third computes the time variations after increasing the number of nested geometries present in the composite solid.

2 Related Works

We discuss below the techniques most related to ours. However, there is a tremendous body of work in this area and we; therefore, cannot possibly provide an absolute overview. Our goal is instead to outline similarities and differences with some of the widely adopted approaches for CSG modeling.

Constructive solid geometry has been a subject of study since the late 1970s. It was initially introduced in [22] as a digital solution to help in the design and production activities in the discrete goods industry, this marked the basis for formalizing the method.

A rigorous mathematical foundation of constructive solid geometry was later laid out in [15]. The membership classification function, a generalization of the ray clipping method used in CSG, is also thoroughly discussed and various formal properties are introduced.

A few years later it was revisited in [17] where Roth et al. (1982) introduced ray casting as a basis for CAD solid modeling systems. Challenges of adequacy and efficiency of ray casting are addressed, and fast picture methods for interactive modeling are introduced to meet the challenges.

The focus then turned towards different optimizations of CSG algorithms in the setting of ray tracing. A simplistic and more elegant single hit intersection algorithm is introduced in [7]. This suggested mechanism reduces memory load and the number of computations performed to perform ray classification. Though limitations have to be respected since sub-objects must closed, non-self-intersecting, and have consistently oriented normals.

A ”slicing” approach is also proposed in [11]. Similar to our proposed solution combinations of meshes and analytical primitives through CSG operations are permissible. Nevertheless, this approach requires one boolean per primitive and a complete evaluation of the CSG expression; therefore, making it simple but limited, and much better approaches are imaginable.

Bound definitions are also a popular way of significantly reducing the time required by CSG algorithms. If the ray and the geometric entities are bound, we perform one first test to see if the ray and the box around a geometric entity overlap. Only if the boxes overlap does one continue to test to determine whether the ray and the entity overlap. A submitted S-bounds algorithm is brought forth in [4] as a means of acceleration in the solid modeling and CSG.

Techniques that optimize various CSG rendering algorithms, namely the Goldfeather and the layered Goldfeather algorithm, and the Sequenced-Convex- Subtraction (SCS) algorithm are advanced in [8]. Although the work represents a significant improvement towards real-time image-based CSG rendering for complex models, the main focus is on hardware acceleration.

3 Constructive Solid Geometry

3.1 Ray Intersection

Ray intersection is the essence of all ray tracing systems. We supply the system a ray as input and obtain knowledge on how the ray intersects solids in the scene as an output. In ray casting engines, one only necessitates computing the nearest intersection to assess the given scene. However, when evaluating CSG models, we require both the closest and furthest intersections to arrange the ray intersections. With knowledge of all the information in the scene - essentially the camera model and the solids - an evaluation of the closest and most distant intersection is executed with each returning the latter information:

$\vec{o}$ = is the origin of the ray (i.e: origin of the camera model).
$\vec{d}$ = is the direction of the ray (i.e: direction from camera origin to pixel in screen).
t = the distance to either the closest or furthest intersection.
$prim$ = a pointer holding surface information of the intersected primitive.

We can distinguish two types of ray intersections. Firstly, ray-primitive intersection tests on convex primitives such as blocks, cylinders, cones, spheres. Because the primitives are analytically defined, the solution is solving the analytic intersection equation. Consequently, this means that the intersection solution is primitive-specific. Many resources providing the analytical solutions are available [14]. Second, we encounter the more generic solid-primitive intersection. As we have previously defined in the introduction, a solid is often a boundary representation composed of several triangles. Hence, the main intricacy in ray-solid intersection renders iterating over all primitives and reducing the problem to ray-primitive intersection tests such that the primitives are triangles - polyhedra more abstractly. We can consider the ray-solid intersection as a more general form of ray-primitive intersection since a primitive is always representable as a solid bearing a single surface. The interesting consequence of such an abstraction is that if we fire a ray in the scene, the computation for determining ray intersection is:

Algorithm 1: Ray-solid furthest and closest intersection.

```
Result: [in, out] intersection range
initialization;
for every primitive in the solid do
    solve the ray-primitive equations;
    if intersection exists then
        if current intersection is closer than in then
            set in to current intersection;
        if current intersection is further than out then
            set out to current intersection;
end
```

The ray-solid intersection test has four possible outcomes (also see Figure **??**):

1. The ray misses the solid.
2. The ray is tangent to the solid.
3. The ray enters and exists the solid.
4. The ray is inside/on the face of a solid and has one intersection.

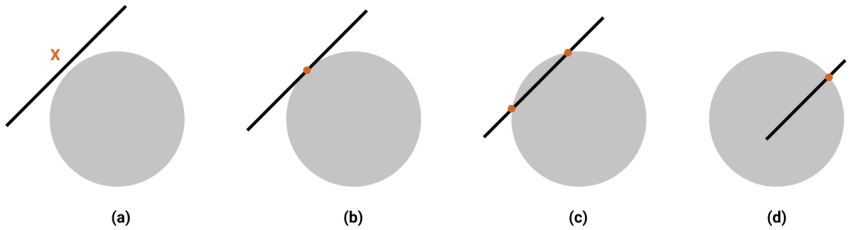

Figure 5: Different ray intersection cases shown on a disk.

The first case is self-evident. The second case is also considered as a no intersection result. In case 3, we compute both the entering and exiting points. Case 4 is more

interesting as we automatically consider the intersection as "double in", this has some interesting implications which will be discussed in Section 3.4. Since we can now retrieve both $[in, out]$ ray-solid intersection, we can move to the second essential part of our CSG evaluation.

3.2 Mathematical Formulations

We will be treating a few mathematical formulations as one cannot design a reliable geometric algorithm in the absence of a clear mathematical statement of the problem to be solved. Topology and set theory have been intensively discussed previously in [15], [20], and other textbooks [10]. Therefore, we will be mainly focusing on definitions and properties that interest us. Formal proofs of the introduced properties are also available in the before-mentioned resources. Constructive solid geometry is based largely on modern Euclidean geometry and the general topology of subsets of three-dimensional Euclidean space E^3.

3.2.1 Set Algebra

Definition 3.1 (Set Operations)**.** Assume that X and Y are subsets of a universe W. We can use the following standard notations:

$$X \cup Y \tag{1}$$
$$X \cap Y \tag{2}$$
$$X - Y \tag{3}$$

Where (1), (2), and (3) denote the union, intersection, and difference of the subsets X and Y respectively. [12]

Property 3.1. *Union and intersection operations are commutative. [12]*

$$X \cup Y = Y \cup X$$
$$X \cap Y = Y \cap X$$

Property 3.2. *Union and intersection operations are distributive over themselves and each other. [12]*

$$X \cup (Y \cap Z) = (X \cup Y) \cap (X \cup Z)$$
$$X \cap (Y \cup Z) = (X \cap Y) \cup (X \cap Z)$$

Property 3.3. *The empty set $\emptyset$ and the universe W are identity elements for the union and intersection operators. [12]*

$$X \cup \emptyset = X$$
$$X \cap W = X$$

Property 3.4. *The complement, denoted c, satisfies [12]:*

$$X \cup cX = W$$
$$X \cap cX = \emptyset$$

[12]

Definition 3.2. A set of elements from the universe W plus the three operators $\cup$, $\cap$, and $-$ that satisfy the properties (3.1) to (3.4) is called boolean algebra [15].

3.2.2 Topological Spaces

Topological spaces are a generalization of metric spaces in which the notion of "nearness" is introduced but not in any quantifiable way that requires a direct distance definition.

Definition 3.3 (Topological Space)**.** A topological space is a pair (W, T) where W is a set and T is a class of subsets of W called the open sets and satisfying the following three properties:

Property 3.5. *The empty set $\emptyset$ and the universe W are open.[12]*

Property 3.6. *The intersection of a finite number of open sets is an open set. [12]*

Property 3.7. *The union of any collection of open sets is an open set. [12]*

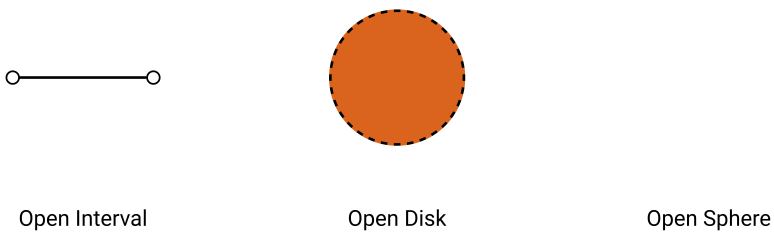

Figure 6: A representation of different open sets of varying dimensional order.

3.2.3 Closed Sets

Definition 3.4 (Closed Sets)**.** A subset X of a topological space (W, T) is closed if its complement is open. However, this don't mean that closed sets are the opposite of open sets (e.g. the universe W and the null set $\emptyset$ are both open and closed). Closed sets hold the following properties which are duals of properties (3.5) to (3.7).

Property 3.8. *The empty set $\emptyset$ and the universe W are closed. [12]*

Property 3.9. *The union of a finite number of closed sets is a closed set. [12]*

Property 3.10. *The union of a finite number of closed sets is a closed set. [12]*

3.2.4 Interior

Definition 3.5. A point of x of W is an interior point of a subset X of W if X is a neighborhood of x. The interior of a subset X of W, denoted iX, is the set of all the interior points of X. [15]

3.2.5 Boundary

Definition 3.6. A point x of W is a boundary point of a subset X of W if each neighborhood of x intersects both X and cX. The boundary of X, denoted bX, is the set of all

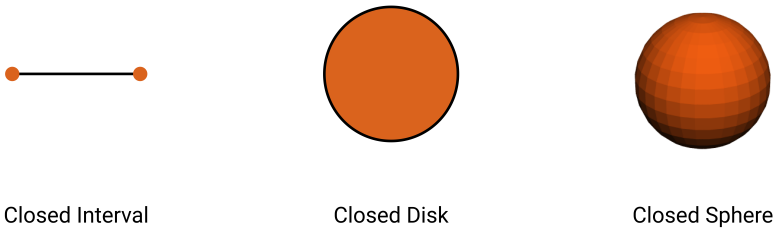

Figure 7: A representation of different closed sets of varying dimensional order.

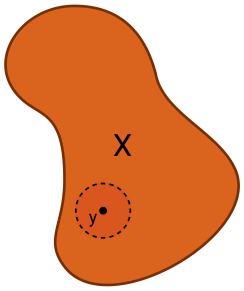

Figure 8: Interior point y on a subset X.

boundary points of X. [15]

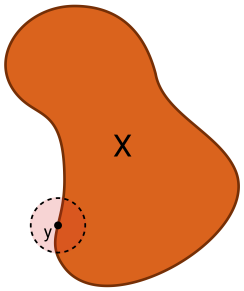

Figure 9: Boundary point y on a subset X.

3.2.6 Closure

Definition 3.7. The closure of a subset X, denoted kX, is the union of X with the set of all its limit points. A point is a limit point of a subset X of a topological space (W, T) if each neighborhood of x contains at least a point of X different from x. [15]

3.2.7 Regularity

Definition 3.8 (Regularity)**.** The regularity of a subset X of W, denoted rX, is the set of $rX = kiX$. [12]

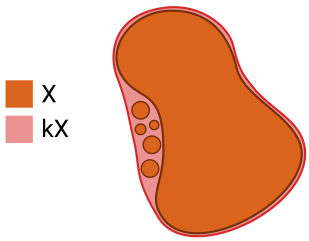

Figure 10: Closure kX of a subset X.

Definition 3.9 (Regular Set)**.** A set X is regular if $X = rX$, i.e. if $X = kiX$. [12]

Definition 3.10 (Regularized Set Operators)**.** The regularized union, intersection, difference and complement are defined per:

$$X \cup^* Y = r(X \cup Y)$$
$$X \cap^* Y = r(X \cap Y)$$
$$X -^* Y = r(X - Y)$$
$$c^x X = rcX$$

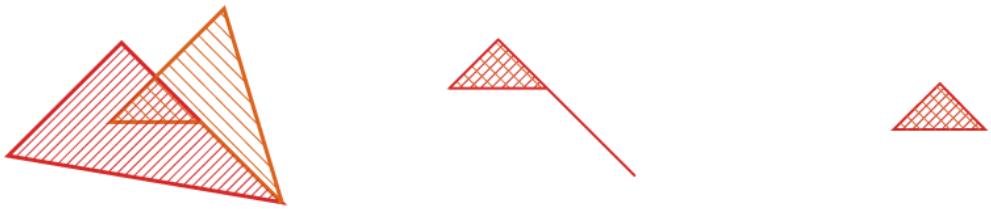

(a) Initial Polygons (b) Normal Intersection (c) Regular Intersection

Figure 11: Normal polygon intersection versus regularized intersection.

3.2.8 Membership Classification Function

The membership classification function allows to segment a candidate set into three subsets which are the ”inside”, ”outside”, and ”on the” of the reference set. Here, we will abstractly define what membership classification before moving to the practical implementations and implications of the more specific ray classification. This theory depends heavily on the previously defined notions of interior, closure, boundary, and regularity. For a brief recapitulation, a point p is an element of the interior of a set X, denoted iX, if there exists a neighborhood of p that is contained in X; p is an element of the closure of X, kX, if every neighborhood of p contains a point of X; p is an element of the boundary of X, bX, if p is an element of both kX and $k(cX)$, where c denotes the complement. A set is said to be regular if $X = kiX$.

The membership classification function works on a pair of point sets:

S = The regular reference set in a subspace W.
X = The candidate regular set X, classified with respect to S, in a subspace W' of W.

Table 1: Notation

E^n	Euclidean n-space
$\emptyset$	Empty Set
W	Reference Set Universe
W'	Candidate Set Universe
$\cup, \cap, -, c$	Set Operators
$\cup^*, \cap^*, -^*, c^*$	Regularized Set Operators in W
$\cup^{*'}, \cap^{*'}, -^{*'}, c^{*'}$	Regularized Set Operators in W'
i, b, k, r	interior, boundary, closure, and regularity in W
i', b', k', r'	interior, boundary, closure, and regularity in W'

Primed symbols will be used in order to denote operations on the subspace W' while normal symbols will be used to denote the subspace W: see table 1.

Definition 3.11. The membership classification function, $M[]$ is defined as follows:

$$M[X, S] = (XinS, XonS, XoutS). \tag{4}$$

where

$$XinS = X \cap^{*'} iS$$
$$XonS = X \cap^{*'} bS$$
$$XoutS = X \cap^{*'} cS$$

The results obtained from this classification $(XinS, XonS, XoutS)$ are the regular portions of the candidate set, X, in the interior, boundary, and the exterior of the reference set W: see figure 12. The classification results also reflect a few properties. The produced results are a quasi-disjoint decomposition of the candidate; therefore:

$$X = XinS \cup XonS \cup XoutS \tag{5}$$

and for "almost" all points in the subset:

$$XinS \cap XonS = \emptyset$$
$$XonS \cap XoutS = \emptyset$$
$$XinS \cap XoutS = \emptyset$$

We say almost since the subsets are generally not disjoint in the conventional sense. (e.g. in figure 5 $XinS$ and $XonS$ share a boundary point).

3.2.9 Classification by constructive geometry

Constructive geometry representations are binary trees whose nonterminal nodes designate regularized set operators and whose terminal nodes designate primitives. We refer to the specific case of constructive geometry in E^3 where regularized compositions are constructed of solid primitives as Constructive Solid Geometry. Regular sets are closed under the regularized set operators thus a class of regular sets can be represented constructively as a combination of other more simple (regular) sets.

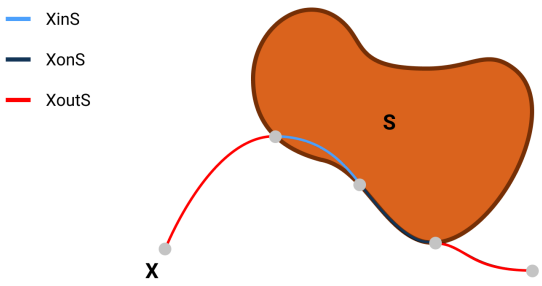

Figure 12: Membership classification function.

For example, as illustrated in Fig. 13, if the universe W is in E^2 and we select the class of closed half-planes as our primitives, we could construct any regular set in E^2 given that it is bounded by a finite number of straight line segments.

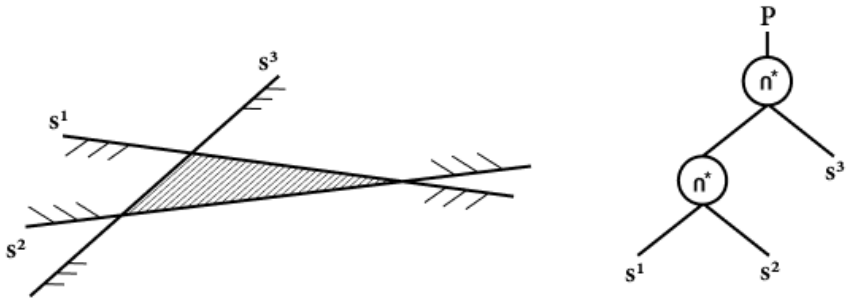

Figure 13: A constructive representation of a polygon P using half-planes. The tree on the right is the constructive geometry representation.

We choose to define the constructively represented regular sets using the divide-and-conquer paradigm as it is a natural approach to to compute the value of such a function. Therefore, when a regular set S is not a primitive, a nonterminal node, we convert the problem of evaluating the function $f(S)$ into two simpler instance of f evaluation followed by a combine, g, step. When S is a primitive, a terminal node, the problem can no longer be divided and an evaluator, e-f, is used. We can now consider the general algorithm for evaluation $M[]$ when the reference set S is represented constructively.

$$M[X,S] = \begin{cases} \text{e-}M(X,S), & \text{if } S \subset A \\ g(M[X,\text{l-subtree}(S)], M[X,\text{r-subtree}(S)], \text{root}(S)), & \text{otherwise} \end{cases} \quad (6)$$

where

e-M	=	The primitive evaluation function.
A	=	The set of all allowed primitives.
g	=	The combine function.
l-subtree	=	The left subtree.
r-subtree	=	The right subtree.
root	=	The operation type. [1]

To customize this general definition to be used in a specific domain, one must design the primitive classification procedure, e-M, and the combine procedure, g. We have already defined our primitive classification procedure in section 3.1. The combine procedure is discussed thoroughly in the next section.

3.3 Ray classification

Given a ray and a solid composition tree, our procedure classifies the ray with respect to the solid and returns the classification to the caller. As previously defined, the classification of a ray with respect to a solid is the information describing the closest and furthest ray-solid intersection, $[in, out]$. The procedure starts at the top of the solid composition tree, recursively descends to the terminal nodes, classifies the ray with respect to the primitives, and then returns the tree combining the classifications of the left and right subtrees. Therefore, if our classification runs on a tree with depth 1, we would receive an $[in, out]$ for each of the solids in the root nodes. Depending on which case operation it is, we might or might not receive either or both the in and the out. (E.g: if the ray is tangent to a solid, then one only receives the in). As illustrated in 14, we can compute the combinations of the pair of intersections we have which in its core is a matter of boolean algebra, see table 2. An important note is that in the case of matching ins or outs, one must always pick the one that is closest to the origin of the ray.

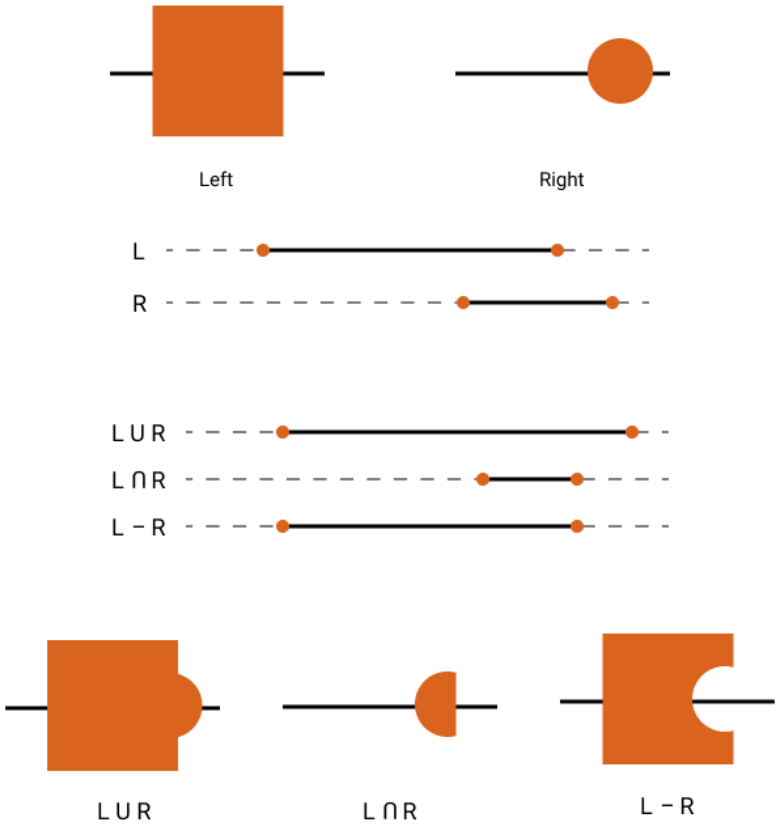

Figure 14: Example of combining ray classifications.

[1]The current node always contains the operation.

Table 2: Boolean operations table

Set Operator	Left Solid	Right Solid	Composite
$\cup$	in	in	in
	in	out	in
	out	int	in
	out	out	out
$\cap$	in	in	in
	in	out	out
	out	in	out
	out	out	out
$-$	in	in	out
	in	out	in
	out	in	out
	out	out	out

4 Optimization

In this section, we will introduce the state-of-the-art CSG algorithm that is implemented in the OpenRT framework. Here we expose all the adjustments and changes we have made to the algorithm in order to maximize its performance and results. First, we will discuss box enclosures, their limitations, and how we simple techniques such as ”early-outs” can increase the performance. We will discuss the binary space partition tree acceleration and spatial indexing structure, including a modified version in order to optimally reverse the tree traversal. Finally, we will put it all together in our version of the CSG algorithm.

4.1 Minimal hit CSG classification

What we have introduced in the previous section is the typical approach to rendering CSG. However, this approach could be very costly as we nest more geometries in the tree and requires a lot of memory to store, classify, and combine a long chain of operations and primitives. Therefore, we introduce a new approach which we refer to as minimal hit CSG classifications. The approach described here computes intersections with binary CSG objects using the single nearest intersections whenever possible. Though it may need to do several of these per sub-object, the number needed is quite low. To our knowledge, this approach was entirely developed in OpenRT and no resources found describe this type of ray classifications. Though a relatively similar algorithm has been introduced in [7], it was proven in [23] to not be functional for the intersection and difference operations. Additionally, the previously mentioned algorithm also heavily relies on surface normals in order to determine the position of the ray. However, one could argue that normals are not always a reliable measure especially when allowing the use of BREPs in the tree since meshes tend to suffer from degeneracy and badly oriented normals.

Table 3: Notation

A, B	left sphere, right sphere.
t_A, t_B	Current ray intersection distance with A, B.
min_A, min_B	Closest ray intersection distance with A, B.
max_A, max_B	Furthest ray intersection distance with A, B.
P_A, P_B	Intersection point such that $\vec{P} = \vec{o} + t\vec{d}$ for A, B..

4.1.1 Union Classification

Consider the case of a simple union of two sphere shown in Figure 15. The union of these two spheres is the the boundary of each of the spheres without their interior. Therefore, to find the correct classification results we must find the closest intersection from our ray origin such that it does not belong to the interior of the sphere. Our ray tracer can find this out by shooting a ray at each of the objects. Let us denote the intersection distance from the ray origin to the point as t_A such that $t_A > min_A$ and $t_A < max_A$. $\vec{P_A}$ is the intersection point which we can compute through the general ray equation $\vec{P_A} = \vec{o} + t\vec{d}$, see Table 3. Initially, min_A is set to $+\inf$, and max_A is set to $-\inf$. Additionally, min_A takes the value of t_A if and only if $t_A < min_A$. Meanwhile, max_A takes the value of t_A if and only if $t_A > max_A$.

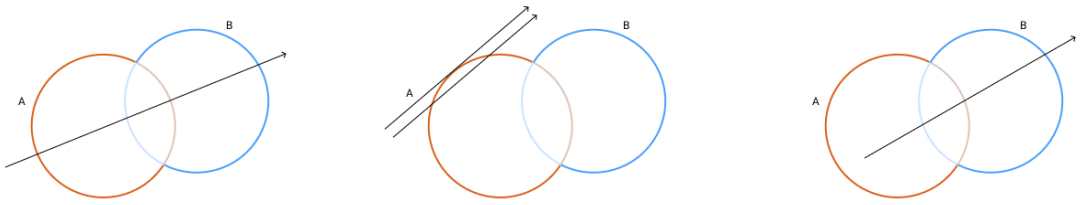

(a) Ray goes through both spheres.

(b) Ray misses one of the spheres.

(c) Ray is inside one of the spheres.

Figure 15: Union ray classification cases.

For the case in Figure 15a, one would simply have to find $MIN(min_A, min_B)$ in order to determine which one of the spheres boundaries is closest.

Let us now consider the case where no intersection is found with one or all of the solids as shows in Figure 15b. In case the ray only hits one of the boundaries, then the previous evaluation $MIN(min_A, min_B)$ still holds as it would return the closest of the two distances, min_A, since t_B was initially set to $+\inf$. Of course, if there was no intersection with both A or B, then there can't be an intersection with their union.

As illustrated in 15c, the last case is if the ray is shot from inside of the solid. This is more complicated since we have to teach our ray tracer to ignore the interior sides and only get the outer sides. Since so far we only check for the min intersections, we will now have to also find the furthest intersection of A and B. This can lead to 2 cases. If the ray only misses the boundary of solid A but intersects every other interior and boundary, then we must check if $max_A > min_B$. In that case, we can return max_B as the correct intersection point since that means the two spheres do actually share interior area. However, if $max_A < min_B$ then the spheres are far away from each other and we can automatically pick max_A as our intersection. The algorithm defined below summarizes

the minimal hit classification for the union operation 2.

Algorithm 2: Minimal hit classification for union.

Result: t intersection distance
min_A = intersectMin(A);
min_B = intersectMin(B);
if $min_A != \inf$ *and* $min_B != \inf$ **then**
  return $MIN(min_A, min_B)$;
if $min_A != \inf$ *and* $min_B == \inf$ **then**
  max_B = intersectMax(B);
  if $max_B = -\inf$ **then**
    return min_A;
  if $max_B < min_A$ **then**
    return max_B;
  max_A = intersectMax(B);
  return max_A;
if $min_a == \inf$ *and* $min_b != \inf$ **then**
  max_A = intersectMax(A);
  if $max_A == -\inf$ **then**
    return min_B;
  if $max_A < min_B$ **then**
    return max_A;
  max_B = intersectMax(B);
  return max_B;
if $min_A == \inf$ *and* $min_B == \inf$ **then**
  max_A = intersectMax(A);
  max_B = intersectMax(B);
  if $max_A == -\inf$ *and* $max_B == -\inf$ **then**
    return $miss$;
  return $MAX(max_A, max_B)$;

4.1.2 Intersection Classification

We will stick to the same general example; however, we will be performing the intersection of two spheres as shown in Figure 16.

Contrary to the union, the intersection of two spheres is their interior without the boundary of each of the spheres. We will use the same previously defined notations shown in Table 3. First, we will start with the obvious case where a ray completely goes through both A and B, as shown in Figure 16a. We first only compute the min_A and min_B as it is the first case we generally would like to check for. If both min_A and min_B are their default values, $+\inf$, then that means the ray completely misses both of the spheres and need not to compute the intersection. However, if both min_A and min_B have values different to the default then we are sure our ray is indeed going through both the spheres; therefore, we would check for the furthest one of both and return that as we are only interested in the interior.

The second case is when a ray only intersects with one of the spheres, as illustrated in Figure 16b. By definition, the intersection operation is the shared section of the sets; therefore, if a ray only intersects one the two spheres then an intersection doesn't exist

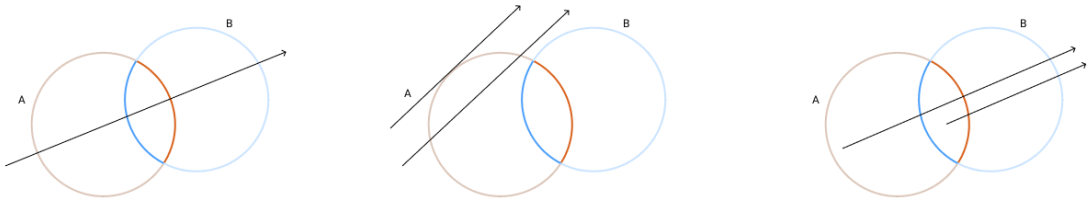

(a) Ray goes through both spheres.

(b) Ray misses one of the spheres.

(c) Ray is inside one or both spheres.

Figure 16: Intersection ray classification cases.

and we should return a miss. However, in the case where the ray enters A but doesn't enter B, an edge case might arise. If the ray is shot in the direction from B to A, and the ray lies inside of the sphere B, then this case would also initially return that the ray enters A but doesn't enter B, this case will be dealt with in the next paragraph but for now this means that we are obliged to check if the ray intersects with B at all. Therefore, we must now compute the furthest intersection, max_B. If B doesn't have a furthest intersection, then we can be sure that the ray entirely misses that sphere and return a miss. Otherwise, we move to the next case.

The last case is when the sphere is inside one or both of the solids. The first case arises when the ray doesn't enter A but enters B. As this could also be mistaken for the case where a ray following the direction from B to A enters B but misses A, we must again check if this ray hits A at all by computing the furthest intersection. If it exists, then we return the entering ray intersection from A. If it doesn't, then we must return a miss. Another case is when the ray is shot from inside the shared interior of A and B. This means the ray doesn't enter A and B but only exits both of them. Here we must compute the exits of A and B and return the closest one of both. If the ray misses one of the exits then the ray entirely misses one the spheres and we can consider this as a miss (we already know it didn't enter any of them). Algorithm 3 showcases the different cases in pseudo code.

4.1.3 Difference Classification

Difference remains the most complex and least optimizable operation out of all three due to several factors. First, the minimal knowledge of the scene is higher than both previously mentioned operations. Second, the difference operations are not commutative nor distributive; therefore, the direction of the ray renders completely different results. We shall stick to the same example as the previous two cases and with similar notations. See Figure 17. We introduce two new notations $d1$ and $d2$, a reference to the direction of the rays. Such that $d1$ is the direction of the ray going from A to B and vice-versa. The difference highlighted in this section is $A-B$; thus, we are interested in the boundary of A that is not part of the interior of B, and the interior of B with respect to A.

We will first consider the case where a ray misses one of the two spheres, as shown in Figure 17a. Contrary to union and intersection, we always get both the closest and furthest intersection points of A. If the ray does not enter or exit A, we can already consider this a miss ($d2$ in Fig. 17a). However, if it either enters or exits A, we must already review if it enters B, thus we compute min_B. If the ray doesn't enter B, we return the shortest of the two distances min_A and max_A. Otherwise, we move to the next case.

Algorithm 3: Minimal hit classification for the intersection.

Result: t intersection distance
min_A = intersectMin(A);
min_B = intersectMin(B);
if $min_A != \inf$ *and* $min_B != \inf$ **then**
  return $MAX(min_A, min_B)$;
if $min_A != \inf$ *and* $min_B == \inf$ **then**
  max_B = intersectMax(B);
  if $min_A < max_B$ **then**
    return min_A;
  return $miss$;
if $min_A == \inf$ *and* $min_B != \inf$ **then**
  max_A = intersectMax(A);
  if $min_B < max_A$ **then**
    return min_B;
  return $miss$;
if $min_A == \inf$ *and* $min_B == \inf$ **then**
  /* Note that the choice of which max to compute first is arbitrary. */
  max_A = intersectMax(A);
  if $max_A == -\inf$ **then**
    return $miss$;
  max_B = intersectMax(B);
  if $max_B == -\inf$ **then**
    return $miss$;
  return $MIN(max_A, max_B)$;

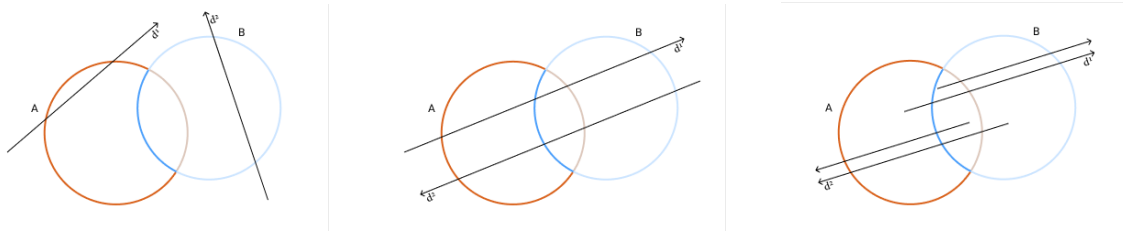

(a) Ray misses one of the spheres.

(b) Ray goes through both spheres.

(c) Ray is inside one or both spheres.

Figure 17: Intersection ray classification cases.

As illustrated in 17b, this case heavily depends on the direction of the ray. Starting with ray $d1$, if we have completed the first check of entering and exit of A we can move to check B. We now need both the entrance and exit points of B. Assuming Bs points are both not the default values ($\pm\inf$), we must first check if $min_A < min_B < max_B$. If this holds, then we can already return the entry point of B as our intersection. If it doesn't,$d2$ in Fig 17b, and we must then check if $min_B < min_A < max_B < max_A$, then we can return the exit of B as the intersection. This case only stands if all enter and exit points of both A and B are valid.

The last and most complicated case is when the ray lies somewhere inside one of these two spheres. Starting with $d1$, we already understand that the ray doesn't enter but only exists A, thanks to the calculation from the first case. We verify if the ray enters or exits B. If the ray enters and exists B, then we can return min_B. If it only exits B, then we necessitate checking if $max_A < max_B$. If that holds, it is a miss. If it doesn't, we return max_B. However, in the $d2$ case, the ray both enters and exists A but only exits B. We now need to examine if $max_B < min_A$. If that is untrue, then the spheres don't share an interior and are separate from each other; consequently, we return a miss. Nevertheless, if it is true, then we return max_B. Algorithm 5 with all the cases is detailed introduced.

4.2 Bounding Boxes

Bounding boxes are the simplest way to cut down on the number of ray intersection operations and thus reduce the rendering time in general. When used in the context of CSG, the solution implicitly turns into an efficient binary tree traversal. While many other types of enclosures can be used, we use box enclosures for the many advantages they bring. First, an abstract box can be defined by only two points, a maximum and minimum point. Because the enclosure definition will be added to every node in the CSG tree, then we must make sure that we do not increase the needed memory per node. Second, boxes are arguably the tightest types of bounding volumes. Meaning that if a ray-enclosure intersection test is to be done, there is a high chance the ray will also intersect whatever geometry is inside of bounding volume. Lastly, it is relatively straightforward to apply the boolean operations on the bounding boxes while still maintaining a tight boundary around the box and thus also ignoring cases where rays do intersect the primitives in the terminal nodes of the CSG tree but not the composite geometries that are made on a higher level.

An abstract bounding box is a rectangular parallelepiped defined by exactly two points, a minimum point and a maximum point, see Figure 18. Each primitive, solid, and composite must be able to define its own bounding box. For primitive cases, the bounding box is case specific. For example, the bounding box of a primitive sphere of radius $r = 1$ and lo-

Algorithm 4: Minimal hit classification for the intersection.

```
Result: t intersection distance
min_A = intersectMin(A);
max_A = intersectMax(A);
if min_A == inf and max_A == -inf then
    return miss;
min_B = intersectMin(B);
max_B = intersectMax(B);
if min_B == inf and max_A == -inf then
    return MIN(min_A, max_A);
if max_A != -inf and max_B != -inf then
    if min_A != inf then
        if min_B != inf then
            if min_A < min_B and min_B < max_A then
                return min_A;
            if min_B < min_A and max_B < max_A then
                return max_B;
        if min_B == inf then
            if min_A < max_B and max_B < max_A then
                return max_B;
    if min_A == inf then
        if min_B != inf then
            if min_B < max_A then
                return min_B;
        if min_B == inf then
            if max_B < max_A then
                return max_B;
return miss;
```

cated at center point $\vec{o} = (0, 0, 0)$ has a bounding box whose min point is (r, r, r) and max point $(-r, -r, r)$. Solids are a little more complicated since they are composed of many primitives. However, one simply has to create a collapsed bounding box (a bounding box whose min coordinates are $-\inf$ and max coordinates are set to $\inf$) and slowly start inflating by the primitive's predefined boxes. The inflation step is as simple as checking if the value of a coordinate of the current bounding box is smaller or bigger than that of the primitive's bounding box and either picking the smallest or the greatest value depending on the coordinate. For instance, if our current bounding box has $min(0, 0, 0)$ and $max(1, 1, 3)$ and the current primitives bounding box has $min2(-1, -1, 1)$ and $max2(2, 2, 2)$ then the new values of the points of our bounding box become $min(-1, -1, 0)$ and $max(2, 2, 3)$.

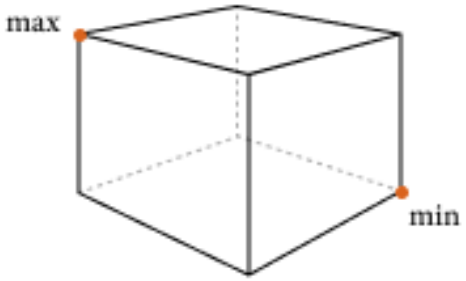

Figure 18: Bounding box.

Combining the boxes on the composite level is also very important to achieve. This can be done trivially using the usual rules of algebra defined in the previous section, except in the case of the difference operation since its results are not as easily predictable and the cost of analyzing the entire composition could be counter-productive in our scenario. In order to apply boolean set operations on a box, we can use the procedure defined in [17]:

Algorithm 5: .

Result: t intersection distance
initialization;
for i = *1, 2, 3* **do**
  if *Operator is* $\cup$ **then**
    min[i] = MIN(leftMin[i], rightMin[i]);
    max[i] = MAX(leftMax[i], rightMax[i]);
  if *Operator is* $\cap$ **then**
    min[i] = MAX(leftMin[i], rightMin[i]);
    max[i] = MIN(leftMax[i], rightMax[i]);
  if *Operator is* $-$ **then**
    min[i] = leftMin[i];
    max[i] = leftMax[i];
end

(target size: 5-10 pages)

5 Evaluation of the results

Summarize the main aspects and results of the research project. Provide an answer to the research questions stated earlier.

(target size: 1/2 page)

6 Conclusion

References

[1] Timo Aila and Samuli Laine. “Understanding the Efficiency of Ray Traversal on GPUs”. In: *Proceedings of the Conference on High Performance Graphics 2009*. HPG ’09. New Orleans, Louisiana: Association for Computing Machinery, 2009, 145–149. ISBN: 9781605586038. DOI: 10.1145/1572769.1572792. URL: https://doi.org/10.1145/1572769.1572792.

[2] Tomas Akenine-Mller, Eric Haines, and Naty Hoffman. *Real-Time Rendering, Fourth Edition*. 4th. USA: A. K. Peters, Ltd., 2018. ISBN: 0134997832.

[3] Arthur Appel. “Some Techniques for Shading Machine Renderings of Solids”. In: *Proceedings of the April 30–May 2, 1968, Spring Joint Computer Conference*. AFIPS ’68 (Spring). Atlantic City, New Jersey: Association for Computing Machinery, 1968, 37–45. ISBN: 9781450378970. DOI: 10.1145/1468075.1468082. URL: https://doi.org/10.1145/1468075.1468082.

[4] S. Cameron. “Efficient bounds in constructive solid geometry”. In: *IEEE Computer Graphics and Applications* 11.3 (1991), pp. 68–74. DOI: 10.1109/38.79455.

[5] Kuang-Hua Chang. *Chapter 3 - Solid Modeling*. Ed. by Kuang-Hua Chang. Boston, 2015. DOI: https://doi.org/10.1016/B978-0-12-382038-9.00003-X. URL: https://www.sciencedirect.com/science/article/pii/B978012382038900003X.

[6] Peter Keenan. *Geographic Information Systems*. Ed. by Hossein Bidgoli. New York, 2003. DOI: https://doi.org/10.1016/B0-12-227240-4/00077-0. URL: https://www.sciencedirect.com/science/article/pii/B0122272404000770.

[7] Andrew Kensler. *Ray Tracing CSG Objects Using Single Hit Intersections*. English. Oct. 2006. URL: http://xrt.wdfiles.com/local--files/doc\%3Acsg/CSG.pdf.

[8] Florian Kirsch and Jürgen Döllner. “Rendering Techniques for Hardware-Accelerated Image-Based CSG.” In: Jan. 2004, pp. 221–228.

[9] Reinhard Klette and Azriel Rosenfeld. *CHAPTER 7 - Curves and Surfaces: Topology*. Ed. by Reinhard Klette and Azriel Rosenfeld. San Francisco, 2004. DOI: https://doi.org/10.1016/B978-155860861-0/50009-2. URL: https://www.sciencedirect.com/science/article/pii/B9781558608610500092.

[10] Alistair H. Lachlan, Marian Srebrny, and Andrzej Zarach. *Set theory and hierarchy theory V: Bierutowice, Poland, 1976*. Springer-Verlag, 1977.

[11] Sylvain Lefebvre. “IceSL: A GPU Accelerated CSG Modeler and Slicer”. In: *AEFA’13, 18th European Forum on Additive Manufacturing*. Paris, France, June 2013. URL: https://hal.inria.fr/hal-00926861.

[12] Maynard J. Mansfield. *Introduction to topology*. R.E. Krieger, 1987.

[13] Stephen M. Pizer et al. *6 - Object shape representation via skeletal models (s-reps) and statistical analysis*. Ed. by Xavier Pennec, Stefan Sommer, and Tom Fletcher. 2020. DOI: https://doi.org/10.1016/B978-0-12-814725-2.00014-5. URL: https://www.sciencedirect.com/science/article/pii/B9780128147252000145.

[14] *Ray tracing primitives*. URL: https://www.cl.cam.ac.uk/teaching/1999/AGraphHCI/SMAG/node2.html (visited on 04/05/2021).

[15] A. Requicha and R. Tilove. “Mathematical Foundations of Constructive Solid Geometry: General Topology of Closed Regular Sets”. In: 1978.

[16] Aristides G. Requicha. “Representations for Rigid Solids: Theory, Methods, and Systems”. In: *ACM Comput. Surv.* 12.4 (Dec. 1980), 437–464. ISSN: 0360-0300. DOI: 10.1145/356827.356833. URL: https://doi.org/10.1145/356827.356833.

[17] Scott D Roth. “Ray casting for modeling solids”. In: *Computer Graphics and Image Processing* 18.2 (1982), pp. 109–144. ISSN: 0146-664X. DOI: https://doi.org/10.1016/0146-664X(82)90169-1. URL: https://www.sciencedirect.com/science/article/pii/0146664X82901691.

[18] Allan D. Spence and Yusuf Altintas. *Modeling Techniques and Control Architectures for Machining Intelligence*. Ed. by C.T. Leondes. 1995. DOI: https://doi.org/10.1016/S0090-5267(06)80031-9. URL: https://www.sciencedirect.com/science/article/pii/S0090526706800319.

[19] Sebastian Steuer. *Methods for Polygonalization of a Constructive Solid Geometry Description in Web-based Rendering Environments*. Dec. 2012. URL: https://www.en.pms.ifi.lmu.de/publications/diplomarbeiten/Sebastian.Steuer/DA_Sebastian.Steuer.pdf.

[20] R.B. Tilove. “A study of GEOMETRIC SET-MEMBERSHIP CLASSIFICATION”. en. (Master’s thesis, University of Rochester, 1977.

[21] *Visualization of a polygon mesh*. Jan. 2021. URL: https://en.wikipedia.org/wiki/Polygon_mesh.

[22] H. B. Voelcker and A. A. G. Requicha. “Geometric Modeling of Mechanical Parts and Processes”. In: *Computer* 10.12 (1977), pp. 48–57. DOI: 10.1109/C-M.1977.217601.

[23] *XRT Renderer*. URL: http://xrt.wikidot.com/doc:csg.